

## Scattering resonances in a degenerate Fermi gas

K. J. Challis, N. Nygaard, and K. Mølmer

*Lundbeck Foundation Theoretical Center for Quantum System Research, Department of Physics and Astronomy, University of Aarhus, DK-8000 Århus C, Denmark*

(Received 26 November 2008; published 6 May 2009)

We consider elastic single-particle scattering from a one-dimensional trapped two-component superfluid Fermi gas when the incoming projectile particle is identical to one of the confined species. Our theoretical treatment is based on the Hartree-Fock ground state of the trapped gas and a configuration-interaction description of the excitations. We determine the scattering phase shifts for the system and predict Fano-type scattering resonances that are a direct consequence of interatomic pairing. We describe the main characteristics of the scattering resonances and make a comparison with the results of BCS mean-field theory.

DOI: 10.1103/PhysRevA.79.052701

PACS number(s): 03.75.Ss, 03.65.Nk

### I. INTRODUCTION

Scattering experiments have led to many important discoveries in physics. In the field of dilute atomic gases, an understanding of interatomic scattering, as well as scattering between light and atoms, is fundamental to preparing, controlling, and manipulating systems for study. For example, a Feshbach resonance is a two-body scattering resonance that makes it possible to control the strength and sign of interatomic interactions [1]. An understanding of this phenomenon has led to the formation of molecular condensates [2,3] and the investigation of the crossover between Fermi superfluidity and Bose-Einstein condensation [4,5].

Our interest is in collective aspects of quantum collisions. Degenerate atomic gases open up possibilities for studying collective scattering phenomenon and recently single- or few-particle scattering from a degenerate Bose gas has been considered theoretically [6,7]. We present a theoretical treatment of collective scattering from a two-component degenerate Fermi gas. We imagine the gas confined to one dimension in an optical waveguide [8–10] and localized longitudinally by an additional tight optical trapping potential [11]. To realize the scattering experiment, projectile particles, identical to one of the trapped components, propagate along the waveguide in a well-defined momentum state and collide with the trapped gas.

We describe the elastic-scattering process using a number-conserving theory based on the Hartree-Fock ground state of the trapped gas. We construct the excitations in a configuration-interaction approach using one-particle continuum excitations and bound two-particle one-hole excitations. The excitations are single-particle-like in the asymptotic limit, and we determine the scattering properties of the system by extracting the scattering phase shifts. We predict Fano-type scattering resonances that arise due to the interrelation of the one-particle and the multiparticle branches of the excitation spectrum. In particular, when the energy of a two-particle one-hole bound state lies within the one-particle continuum, coupling between the two branches significantly modifies the scattering properties of the system near the uncoupled bound-state energy. In this system, the two branches of the excitation spectrum are coupled by the interatomic pairing.

We also present a BCS mean-field description of the scattering. In this approach, the scattering properties are determined from the asymptotic behavior of the quasiparticle excitations in the many-body system. We find that, in the uncoupled system, bound hole excitations lie within the particle excitation continuum. It is well known that these bound states acquire a width in the presence of the mean-field pair potential (e.g., [12] and references therein) and we again observe Fano-type scattering resonances. However, these resonances are quantitatively different from those predicted by the configuration-interaction method. In this particular system, the BCS treatment leads to spurious results that are explicitly linked with the violation of particle number conservation in the theory. Effects of this type are particularly evident in small systems.

Our paper is organized as follows. In Sec. II we outline the system for study. In Sec. III we investigate elastic single-particle scattering from a trapped Fermi gas using the configuration-interaction method. In Sec. IV we present the BCS mean-field treatment of that same problem. In Sec. V we give a detailed discussion of the validity of the mean-field approach, and we conclude in Sec. VI.

### II. TWO-COMPONENT FERMION GAS

We consider a trapped one-dimensional degenerate Fermi gas at zero temperature with two equally populated spin components interacting weakly via an attractive contact potential. The Hamiltonian is

$$\hat{H} = \sum_{\alpha} \int \hat{\psi}_{\alpha}^{\dagger}(x) H_{\text{SP}}(x) \hat{\psi}_{\alpha}(x) dx + g \int \hat{\psi}_{\uparrow}^{\dagger}(x) \hat{\psi}_{\downarrow}^{\dagger}(x) \hat{\psi}_{\downarrow}(x) \hat{\psi}_{\uparrow}(x) dx, \quad (1)$$

where the field operator  $\hat{\psi}_{\alpha}(x)$  destroys a particle at position  $x$ , in the spin state  $\alpha = \uparrow, \downarrow$ , and  $g < 0$ . The single-particle Hamiltonian is

$$H_{\text{SP}}(x) = -\frac{\hbar^2}{2M} \frac{d^2}{dx^2} + V_{\text{ext}}(x), \quad (2)$$

where  $M$  is the atomic mass and  $V_{\text{ext}}(x)$  is a symmetric external trapping potential with a zero energy continuum

threshold. The exact form of the trapping potential is not crucial for our discussion. However, for our numerical calculations we use the Gaussian form  $V_{\text{ext}}(x) = -V_0 \exp(-2x^2/w^2)$ , with  $V_0 > 0$ , which can be realized experimentally for atoms in a waveguide by applying a single Gaussian laser beam. The Gaussian width provides a convenient energy scale  $E_w = \hbar^2/2Mw^2$ .

### III. CONFIGURATION-INTERACTION METHOD

To describe elastic single-particle scattering we determine the excitation spectrum using the equation of motion method [13]. The ground state  $|G\rangle$  of the trapped gas has energy  $\mathcal{E}_G$ , i.e.,  $\hat{H}|G\rangle = \mathcal{E}_G|G\rangle$ . We introduce the operators  $\hat{Q}_\nu^\dagger$  that create excitations  $|\nu\rangle = \hat{Q}_\nu^\dagger|G\rangle$  satisfying  $\hat{H}|\nu\rangle = \mathcal{E}_\nu|\nu\rangle$ , and the excitation spectrum is given by

$$[\hat{H}, \hat{Q}_\nu^\dagger]|G\rangle = \bar{\mathcal{E}}_\nu \hat{Q}_\nu^\dagger|G\rangle, \quad (3)$$

where  $\bar{\mathcal{E}}_\nu = \mathcal{E}_\nu - \mathcal{E}_G$ . Projecting Eq. (3) onto the state  $\hat{X}^\dagger|G\rangle$ , where  $\hat{X}$  is an arbitrary operator, gives

$$\langle G|\hat{X}[\hat{H}, \hat{Q}_\nu^\dagger]|G\rangle = \bar{\mathcal{E}}_\nu \langle G|\hat{X}\hat{Q}_\nu^\dagger|G\rangle. \quad (4)$$

Later,  $\hat{X}$  is chosen so that Eq. (4) generates a matrix eigenvalue equation for the excited states  $|\nu\rangle$ . Equation (4) is exact but is difficult to solve because we do not know the ground state  $|G\rangle$  or the excitation creation operators  $\hat{Q}_\nu^\dagger$ .

An approximate solution to Eq. (4) can be found by neglecting pair correlations in the ground state, i.e., we calculate the matrix elements using the Hartree-Fock ground state  $|\text{HF}\rangle$  in place of  $|G\rangle$ . We briefly summarize the Hartree-Fock method here. The Hartree-Fock Hamiltonian is

$$\hat{H}_{\text{HF}} = \sum_\alpha \int \hat{\psi}_\alpha^\dagger(x) [H_{\text{SP}}(x) + W(x)] \hat{\psi}_\alpha(x) dx, \quad (5)$$

where  $W(x) = g \langle \text{HF} | \hat{\psi}_\alpha^\dagger(x) \hat{\psi}_\alpha(x) | \text{HF} \rangle$  is spin independent because we have chosen equal spin populations. The expansion  $\hat{\psi}_\alpha(x) = \sum_n \phi_n(x) \hat{a}_{n\alpha}$  diagonalizes Hamiltonian (5) where the Hartree-Fock wave functions satisfy

$$[H_{\text{SP}}(x) + W(x)] \phi_n(x) = E_n \phi_n(x). \quad (6)$$

The operators  $\hat{a}_{n\alpha}^\dagger$  and  $\hat{a}_{n\alpha}$  obey fermionic commutation relations and the modes are populated according to

$$\langle \text{HF} | \hat{a}_{n\alpha}^\dagger \hat{a}_{n'\beta} | \text{HF} \rangle = n_n \delta_{nn'} \delta_{\alpha\beta}, \quad (7)$$

where, at zero temperature,  $n_n = 1$  for  $E_n < E_F$  and  $n_n = 0$  for  $E_n > E_F$ . We choose the Fermi energy  $E_F < 0$  so that all of the particles are bound. The Hartree-Fock ground state is constructed by adding one particle of each spin to the lowest available energy level until the Fermi energy is reached, i.e.,

$$|\text{HF}\rangle = \left( \prod_{n \leq n_F} \hat{a}_{n\uparrow}^\dagger \hat{a}_{n\downarrow}^\dagger \right) |0\rangle, \quad (8)$$

where  $n_F$  denotes the highest occupied level.

We determine the Hartree-Fock ground state of the system by numerically calculating the self-consistent Hartree poten-

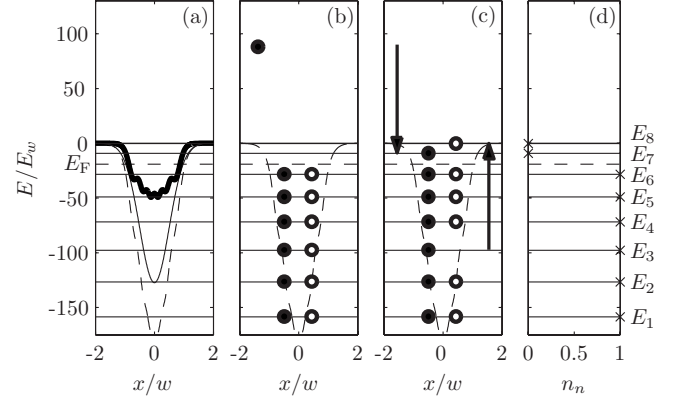


FIG. 1. (a) The Hartree-Fock ground state of a trapped Fermi gas. The curves correspond to (thick) the Hartree potential  $W(x)$ , (thin) the Gaussian external potential  $V_{\text{ext}}(x)$ , and (dashed) the combined potential  $V_{\text{ext}}(x) + W(x)$ . (b) A scattering one-particle excitation and (c) a bound two-particle one-hole excitation, where the energy-level occupation of the (●) spin-up and (○) spin-down particles is indicated schematically. The arrows indicate the particle rearrangement between the configurations in panels (b) and (c). (d) The ground-state energy-level occupation [see Eq. (7)] is indicated by the horizontal component of the markers  $\times$ . In all panels, the horizontal lines indicate (dashed) the Fermi energy  $E_F$  and (solid) the bound Hartree-Fock energies  $E_n < 0$  [see Eq. (6)]. Parameters are  $g = -9.55wE_w$ ,  $V_0 = 127.32E_w$ , and  $E_F = -19.10E_w$ .

tial  $W(x)$ . We use an iterative method where the kinetic-energy term in Eq. (6) is evaluated according to a finite-difference formula. Figure 1(a) shows the Hartree potential for a particular set of parameters where there are six particles of each spin state, i.e.,  $\langle \hat{N}_\alpha \rangle = \int \langle \hat{\psi}_\alpha^\dagger(x) \hat{\psi}_\alpha(x) \rangle dx = 6.00$ . We have chosen to consider a small number of particles so that identifying the scattering features is straightforward and the breakdown of BCS theory can be demonstrated clearly in Sec. IV. The small particle number means that there are oscillations in the Hartree potential in Fig. 1(a) [14]. In the ground state the particles occupy the lowest available energy levels as shown in Fig. 1(d) [see Eqs. (7) and (8)].

We consider excitations  $|\nu\rangle$  that are single-particle-like in the asymptotic limit but are phase shifted from plane-wave scattering states due to the presence of the external trapping potential and the trapped gas. Formally, the operators  $\hat{Q}_\nu^\dagger$  are constructed from continuum one-particle excitations and bound multiparticle excitations. The multiparticle excitations in general consist of all possible configurations of the particles in the Hartree-Fock energy levels. We include only the leading-order terms, i.e.,

$$\hat{Q}_\nu^\dagger = \sum_q C_q^\nu \hat{a}_{q\uparrow}^\dagger + \sum_{r,s,t} B_{rst}^\nu \hat{a}_{r\uparrow}^\dagger \hat{a}_{s\downarrow}^\dagger \hat{a}_{t\downarrow}, \quad (9)$$

where  $E_q > 0$ , and  $E_r, E_s, E_t < 0$  [15]. The first term in Eq. (9) describes continuum one-particle excitations [e.g., see Fig. 1(b)]. The second term introduces bound two-particle one-hole excitations where the spin of the hole differs from the spin of the projectile particle [e.g., the bound excitation with  $(r, s, t) = (7, 8, 3)$  is illustrated in Fig. 1(c)]. We require  $E_r, E_s > E_F$  and  $E_t < E_F$  as these are the only nonzero contri-

butions when acting on the Hartree-Fock ground state [Eq. (8)].

The coefficients  $C_q^v$  and  $B_{rst}^v$  in Eq. (9) are determined so that Eq. (4) is valid, with  $|G\rangle \rightarrow |\text{HF}\rangle$ . Taking  $\hat{X}^\dagger = \hat{a}_{q\uparrow}^\dagger$  and  $\hat{X}^\dagger = \hat{a}_{r\uparrow}^\dagger \hat{a}_{s\downarrow}^\dagger \hat{a}_{t\downarrow}$  yields

$$E_q C_q^v + \sum_{r,s,t} B_{rst}^v V_{qtsr} = \bar{\mathcal{E}}_v C_q^v, \quad (10)$$

and

$$(E_r + E_s - E_t) B_{rst}^v + \sum_q C_q^v V_{rstq} + \sum_{r',s'} B_{r's't}^v V_{rss'r'} - \sum_{r',t'} B_{r's't'}^v V_{rt'tr'} = \bar{\mathcal{E}}_v B_{rst}^v, \quad (11)$$

respectively, where

$$V_{nmn'n'} = g \int \phi_n^*(x) \phi_m^*(x) \phi_{m'}(x) \phi_{n'}(x) dx. \quad (12)$$

Equations (10) and (11) define a Hermitian eigenvalue problem for the coefficients  $C_q^v$  and  $B_{rst}^v$ . The one-particle continuum excitations ( $C_q^v$ ) are coupled to the bound two-particle one-hole excitations ( $B_{rst}^v$ ) by the full Hamiltonian (1) giving rise to the off-diagonal interaction terms  $V_{qtsr}$ . By construction, the three-particle wave functions associated with the coefficients  $B_{rst}^v$  vanish asymptotically and, in the limit  $x \rightarrow \pm\infty$ , the excitations  $|\nu\rangle$  are described by the single-particle wave functions

$$\Phi_\nu(x) = \sum_q C_q^v \phi_q(x). \quad (13)$$

To investigate the scattering properties quantitatively, the Hartree-Fock ground state is computed on a grid of spatial extent  $2L$ . We invoke the Neumann boundary conditions  $[d\phi_n(x)/dx]_{x=\pm L} = 0$  so that the Hartree-Fock wave functions provide an orthonormal basis. Solving the eigenvalue problem defined by Eqs. (10) and (11), we determine the single-particle wave functions  $\Phi_\nu(x)$  for particular discrete values of the energy eigenvalue  $\bar{\mathcal{E}}_\nu$ . The scattering information at any energy of interest is then extracted using the  $\mathcal{R}$ -matrix method [16], i.e., we match the even and the odd single-particle wave-function solutions to the analytic asymptotic forms

$$\begin{aligned} \lim_{x \rightarrow \pm\infty} \Phi_\nu^e(x) &\propto \cos[kx \mp \delta_e(k)], \\ \lim_{x \rightarrow \pm\infty} \Phi_\nu^o(x) &\propto \sin[kx \mp \delta_o(k)], \end{aligned} \quad (14)$$

where  $\bar{\mathcal{E}}_\nu = \hbar^2 k^2 / 2M$ , and we use the Hartree-Fock basis to reconstruct the asymptotic solutions and the scattering phase shifts  $\delta_e(k)$  and  $\delta_o(k)$ , for any  $k$ .

The even and the odd phase shifts for the trapped Fermi gas considered in Fig. 1 are shown in Fig. 2(a). We observe a variation in the background phase shifts  $\delta_{e,o}^{\text{bg}}(k)$  due to the effective external potential  $V_{\text{ext}}(x) + W(x)$  [see Eq. (6)]. We also observe 24 resonance features that are characterized by a jump of  $\sim \pi$  in either the even or the odd phase shift.

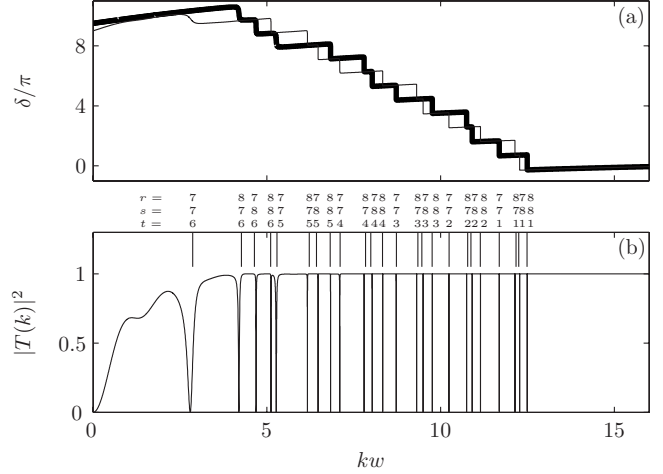


FIG. 2. (a) Scattering phase shifts and (b) transmission probability for a trapped Fermi gas, calculated using the configuration-interaction method. The curves in (a) correspond to (thick) the even phase shift  $\delta_e(k)$  and (thin) the odd phase shift  $\delta_o(k)$ . The vertical lines in (b) indicate the uncoupled resonance wave vectors  $k'_{rs}$  [see Eq. (16)]. Parameters are  $g = -9.55wE_w$ ,  $V_0 = 127.32E_w$ , and  $E_F = -19.10E_w$ .

Transmission and reflection coefficients for the system can be calculated from the phase shifts [6,7]. For a projectile particle incident from  $x = -\infty$  (or equivalently from  $x = \infty$ ), the transmission probability (normalized to one) is given by  $|T(k)|^2 = \cos^2[\delta_e(k) - \delta_o(k)]$ . The transmission probability is shown in Fig. 2(b). As expected,  $|T(k)|^2 \rightarrow 0$  in the limit  $k \rightarrow 0$ , and  $|T(k)|^2 \rightarrow 1$  as  $k \rightarrow \infty$ . The smoothness of the Gaussian external potential means that quantum reflections at the trap edges do not play a significant role. Consequently,  $\delta_e^{\text{bg}}(k) \approx \delta_o^{\text{bg}}(k)$  and the background transmission profile approaches unity without the characteristic oscillations observed in the case of a square-well potential. In addition to the background transmission profile, we observe 24 scattering resonances for which the transmission falls to zero.

The observed scattering resonances are due to interference between the bound two-particle one-hole excitations and the one-particle excitation continuum. The coupling of the two branches of the excitation spectrum is provided by the interatomic pairing, i.e., the matrix elements  $V_{qtsr}$  in Eqs. (10) and (11). For each resonance, the coupling  $V_{qtsr}$  is only nonzero for either the even or the odd continuum wave functions, depending on the parity of the  $(r, s, t)$  bound wave function [see Eq. (12)]. Therefore, a particular  $(r, s, t)$  configuration modifies either the even or the odd continuum states but not both.

The effect on the continuum of an embedded discrete state has been described by Fano [17]. Following that treatment, the resonant phase shift  $\delta_{e,o}^{\text{R}}(k) = \delta_{e,o}(k) - \delta_{e,o}^{\text{bg}}(k)$  near each resonance is approximated by

$$\tan \delta_{e,o}^{\text{R}}(k) = \frac{\Gamma(k)/2}{\bar{\mathcal{E}}_\nu - \mathcal{E}_{rs}^t - \chi(k)}, \quad (15)$$

where the resonance width is  $\Gamma(k) = 2ML|V_{ktsr}|^2 / \hbar^2 k$  and the resonance energy is determined by

$$\mathcal{E}_{rs}^t = \frac{(\hbar k_{rs}^t)^2}{2M} = E_r + E_s - E_t + V_{rssi} - V_{rttr}, \quad (16)$$

and  $\chi(k) = \sum_q |V_{qtsr}|^2 / (\bar{\mathcal{E}}_v - E_q)$ . Taking  $V_{qtsr}$  to be approximately independent of  $q$ , we find that  $\chi(k) = 0$ . The resonance energies are well approximated by  $\bar{\mathcal{E}}_v = \mathcal{E}_{rs}^t$ , as shown by the vertical lines in Fig. 2(b).

The energy  $\mathcal{E}_{rs}^t$  [see Eq. (16)] can be interpreted as the energy required to create the bound two-particle one-hole excitation  $(r, s, t)$ , i.e., to create a spin-up particle in level  $r$  and excite a spin-down particle from level  $t$  to  $s$ . The last two terms in Eq. (16) account for the accompanying change in the pair-wise interaction energy. When the energy of the incoming projectile particle matches  $\mathcal{E}_{rs}^t$ , the bound excitation  $(r, s, t)$  is an allowed intermediate state for the scattering process [see Figs. 1(b) and 1(c) for  $(r, s, t) = (7, 8, 3)$ ]. The intermediate state is made accessible by the two-body coupling term  $V_{qtsr}$  in Eqs. (10) and (11).

#### IV. MEAN-FIELD APPROACH

The BCS mean-field treatment of pairing and superfluidity in fermionic systems has been extremely successful. It is a tractable method that accurately describes a wide range of systems in which fermionic many-body pair correlations are important. One of the features of the BCS approach is that the mean-field pair potential couples the particle and the hole branches of the excitation spectrum, and this means that in finite systems uncoupled bound hole excitations lying in the particle excitation continuum acquire a width [18]. This effect has been studied by a number of authors in the context of pairing in nuclei [12, 19, 20].

In this section we give a pedagogical treatment of elastic single-particle scattering from a two-component degenerate Fermi gas based on the BCS mean-field approach. We identify Fano-type scattering resonances due to deeply bound hole excitations lying in the particle excitation continuum. This scattering problem is particularly useful for a discussion of the validity of BCS mean-field theory because (i) the predicted scattering resonances are extremely sensitive to the ground-state properties of the trapped gas, and (ii) a physical interpretation of the resonances is possible allowing the mean-field approach to be investigated in detail. We broadly follow the organizational sequence of the number-conserving treatment in Sec. III to aid comparison between the two approaches.

In the BCS mean-field treatment, we approximate Hamiltonian (1) by the Hartree-Fock-Bogoliubov Hamiltonian

$$\begin{aligned} \hat{H}_{\text{HFB}} = & \sum_{\alpha} \int \hat{\psi}_{\alpha}^{\dagger}(x) [H_{\text{SP}}(x) + U(x) - \mu] \hat{\psi}_{\alpha}(x) dx \\ & + \int [\Delta(x) \hat{\psi}_{\uparrow}^{\dagger}(x) \hat{\psi}_{\downarrow}^{\dagger}(x) + \text{H.c.}] dx, \end{aligned} \quad (17)$$

where the Hartree potential is  $U(x) = g \langle \hat{\psi}_{\alpha}^{\dagger}(x) \hat{\psi}_{\alpha}(x) \rangle$  and the pair potential is  $\Delta(x) = -g \langle \hat{\psi}_{\uparrow}(x) \hat{\psi}_{\downarrow}(x) \rangle$  [21]. The two spin states are equally populated so  $U(x)$  is spin independent. We choose the chemical potential  $\mu < 0$  so that all of the par-

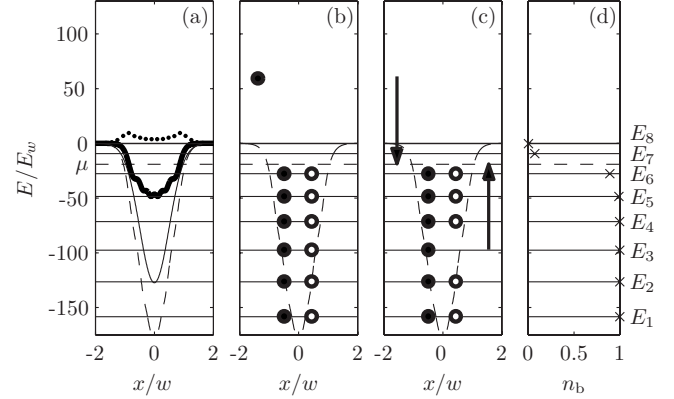


FIG. 3. (a) The BCS ground state of a trapped Fermi gas. The curves correspond to (thick) the Hartree potential  $U(x)$ , (dotted) the pair potential  $\Delta(x)$ , (thin) the Gaussian external potential  $V_{\text{ext}}(x)$ , and (dashed) the combined potential  $\bar{V}(x) = V_{\text{ext}}(x) + U(x)$ . (b) A scattering particle excitation and (c) a bound hole excitation, where the energy-level occupation of the (●) spin-up and (○) spin-down particles is indicated schematically. The arrows indicate the particle rearrangement between the configurations in panels (b) and (c). (d) The ground-state occupation of the bound states in the combined potential  $\bar{V}(x)$  [see Eqs. (20) and (21)] is indicated by the horizontal component of the markers  $\times$ . In all panels, the horizontal lines indicate (dashed) the chemical potential  $\mu$  and (solid) the bound-state energies  $E_n = E_b < 0$  in the combined potential  $\bar{V}(x)$ . Parameters are  $g = -9.55wE_w$ ,  $V_0 = 127.32E_w$ , and  $\mu = -19.10E_w$ .

ticles are bound. The Bogoliubov transformation,

$$\begin{aligned} \hat{\psi}_{\uparrow}(x) &= \sum_n [u_n(x) \hat{\gamma}_{n\uparrow} - v_n^*(x) \hat{\gamma}_{n\downarrow}^{\dagger}], \\ \hat{\psi}_{\downarrow}(x) &= \sum_n [u_n(x) \hat{\gamma}_{n\downarrow} + v_n^*(x) \hat{\gamma}_{n\uparrow}^{\dagger}], \end{aligned} \quad (18)$$

diagonalizes Hamiltonian (17), where the quasiparticle amplitudes  $u_n(x)$  and  $v_n(x)$  solve the Bogoliubov-de Gennes equations [22]

$$\begin{bmatrix} \mathcal{L}(x) & \Delta(x) \\ \Delta^*(x) & -\mathcal{L}(x) \end{bmatrix} \begin{bmatrix} u_n(x) \\ v_n(x) \end{bmatrix} = \epsilon_n \begin{bmatrix} u_n(x) \\ v_n(x) \end{bmatrix}. \quad (19)$$

In Eq. (19),  $\mathcal{L}(x) = H_{\text{SP}}(x) + U(x) - \mu$  and  $\epsilon_n$  are the quasiparticle energies (taking  $\epsilon_n > 0$ ). The quasiparticle operators  $\hat{\gamma}_{n\alpha}^{\dagger}$  and  $\hat{\gamma}_{n\alpha}$  obey fermionic commutation relations, and the quasiparticle modes are populated according to the Fermi distribution function, i.e., at zero temperature,  $\langle \hat{\gamma}_{n\alpha} \hat{\gamma}_{n'\beta}^{\dagger} \rangle = \delta_{nn'} \delta_{\alpha\beta}$  [22].

Figure 3(a) shows the self-consistent BCS mean fields for a trapped Fermi gas. We have used the same parameters as in Figs. 1 and 2. However, in the mean-field treatment, the ground state is not a particle number eigenstate [22]. For the parameters used in Fig. 3, the average number of particles in each spin state is  $\langle \hat{N}_{\alpha} \rangle = 5.97$  and the number variance is  $\langle \hat{N}_{\alpha}^2 \rangle - \langle \hat{N}_{\alpha} \rangle^2 = 0.20$ .



To understand the effect of the off-diagonal coupling in the Bogoliubov-de Gennes equations, we first consider Eq. (19) with  $\Delta(x)=0$ . We retain the Hartree potential  $U(x)$  from the finite  $\Delta(x)$  self-consistent solution. In this case, Eq. (19) reduces to the Schrödinger equation

$$\left[ -\frac{\hbar^2}{2M} \frac{d^2}{dx^2} + \bar{V}(x) \right] \psi_n(x) = E_n \psi_n(x), \quad (20)$$

where  $\bar{V}(x) = V_{\text{ext}}(x) + U(x)$  is the effective confining potential for the many-body system [23]. Equation (20) has discrete bound states  $\psi_b(x)$  with energy  $E_b < 0$ , and an excitation continuum of both even and odd scattering states  $\psi_k^{\epsilon_o}(x)$  with energy  $E_k = \hbar^2 k^2 / 2M > 0$ . In the particle-hole picture, the excitation spectrum has a particle branch [ $u_n^0(x) = \psi_n(x)$ ] with energy  $\epsilon_n^0 = E_n - \mu$  (for  $E_n > \mu$ ) and a hole branch [ $v_n^0(x) = -\psi_n(x)$ ] with energy  $\epsilon_n^0 = -E_n + \mu$  (for  $E_n < \mu$ ). The superscript zero indicates that we are solving Eq. (19) with  $\Delta(x) = 0$ .

Taking  $\Delta(x)$  to be finite introduces coupling between the particle and the hole branches of the excitation spectrum. The quasiparticle excitations then become simultaneously particle-like and hole-like to reflect the fact that the pairing interactions can excite particles to energy levels lying above the chemical potential. Figure 3(d) shows the BCS ground-state average particle occupations of the uncoupled bound states  $\psi_b(x)$ , i.e.,

$$n_b = \sum_n \left| \int \psi_b(x) v_n(x) dx \right|^2. \quad (21)$$

The lowest bound levels are fully occupied but there is a redistribution of particles near the chemical potential, compared to the Hartree-Fock ground state [see Fig. 1(d)].

To investigate the scattering properties of the system, we compute the even and the odd solutions of the Bogoliubov-de Gennes equations [Eq. (19)] subject to Neumann boundary conditions. We then match the asymptotic behavior of the quasiparticle amplitudes to their analytic forms. The even and the odd particle-like amplitudes lying in the continuum have the form

$$\begin{aligned} \lim_{x \rightarrow \pm\infty} u_k^e(x) &\propto \cos[kx \mp \delta_e(k)], \\ \lim_{x \rightarrow \pm\infty} u_k^o(x) &\propto \sin[kx \mp \delta_o(k)], \end{aligned} \quad (22)$$

where  $\epsilon_k = \hbar^2 k^2 / 2M - \mu$ . In the asymptotic limit, the corresponding holelike amplitudes  $v_k^{\epsilon_o}(x)$  tend exponentially to zero. Again we use the  $\mathcal{R}$ -matrix method [16] to determine the scattering phase shifts  $\delta_e(k)$  and  $\delta_o(k)$  for any  $k$ .

The even and the odd phase shifts for the parameters used in Fig. 3 are shown in Fig. 4(a). The phase shifts are independent of the spin of the projectile particle because the two spin states are equally populated. We observe a background variation in the phase shifts due to the effective potential  $\bar{V}(x)$  [see Eq. (20)]. We also observe five resonance features that occur alternately in the even and the odd phase shifts and become narrower higher in the continuum. The transmission probability is shown in Fig. 4(b).

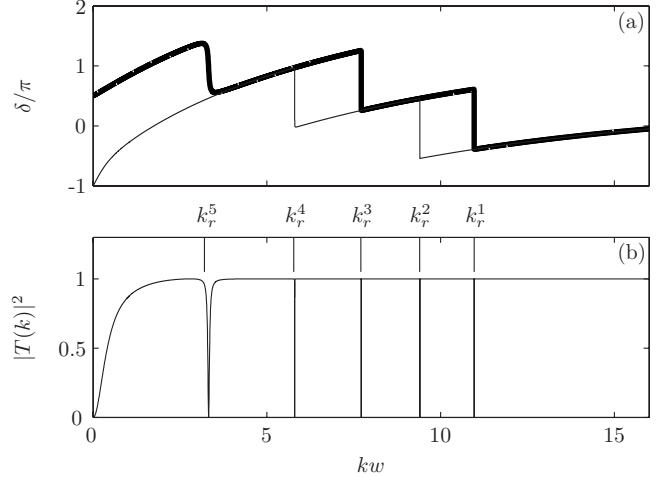


FIG. 4. (a) Scattering phase shifts and (b) transmission probability for a trapped Fermi gas, calculated using the mean-field method. The curves in (a) correspond to (thick) the even phase shift  $\delta_e(k)$  and (thin) the odd phase shift  $\delta_o(k)$ . The vertical lines in (b) indicate the uncoupled resonance wave vectors  $k_r^b$  [see Eq. (23)]. Parameters are  $g = -9.55wE_w$ ,  $V_0 = 127.32E_w$ , and  $\mu = -19.10E_w$ .

The observed scattering resonances are possible because, in the uncoupled system, a scattering particle excitation [e.g., see Fig. 3(b)] can have the same quasiparticle energy as a bound hole excitation [e.g., see Fig. 3(c) for  $b=3$ ]. In particular, a particle scattering state with quasiparticle energy  $\epsilon_k^0 = E_k - \mu$  is degenerate with a bound hole excitation with quasiparticle energy  $\epsilon_b^0 = -E_b + \mu$  when  $\epsilon_k^0 = \epsilon_b^0$ . In the ordinary particle picture this can be rewritten as  $E_k = E_r^b$ , where

$$E_r^b = \frac{(\hbar k_r^b)^2}{2M} = -E_b + 2\mu. \quad (23)$$

If  $E_r^b > 0$ , the uncoupled bound state is embedded in the particle excitation continuum and, when  $\Delta(x)$  is finite, this gives rise to a Fano-type scattering resonance. Note that in Fig. 3 the  $b=6$  bound state does not give rise to a resonance because it does not lie sufficiently low in the trap, i.e.,  $E_6 > 2\mu$ .

Using standard techniques [24], we find that near a resonance the resonant phase shift is well described by the Fano profile

$$\tan \delta_{e,o}^R(k) = \frac{\Gamma_{e,o}(k)/2}{\epsilon_k^0 - \epsilon_b^0 - \chi_{e,o}(k)}. \quad (24)$$

The resonance width is

$$\Gamma_{e,o}(k) = -\frac{2M}{\hbar^2 W_k} Q_{e,o}^2(k) \cos[\delta_e^{\text{bg}}(k) - \delta_o^{\text{bg}}(k)], \quad (25)$$

where  $Q_{e,o}(k) = \int \psi_b(x) \Delta(x) \psi_k^{\epsilon_o}(x) dx$  [25] and the Wronskian  $W_k = \psi_k^o(x) d\psi_k^e(x)/dx - \psi_k^e(x) d\psi_k^o(x)/dx$  is constant because there is no first-order derivative in Eq. (20) [26]. For each resonance, the coupling matrix element  $Q_{e,o}(k)$  is only non-zero for either the even or the odd continuum wave functions, depending on the parity of the bound hole excitation. The smoothness of the Gaussian external potential means

that  $\delta_e^{\text{bg}}(k) \approx \delta_0^{\text{bg}}(k)$  and, therefore,  $\cos[\delta_e^{\text{bg}}(k) - \delta_0^{\text{bg}}(k)] \approx 1$ .

The resonance energy is determined by solving  $\epsilon_k^0 = \epsilon_b^0 + \chi_{e,o}(k)$ , where

$$\chi_{e,o}(k) = \Theta(k) \pm \frac{M}{\hbar^2 W_k} Q_{e,o}^2(k) \sin[\delta_e^{\text{bg}}(k) - \delta_0^{\text{bg}}(k)], \quad (26)$$

and  $\Theta(k) = \int \psi_b(x) \Delta(x) G_k(x, s) \Delta(s) \psi_b(s) dx ds$ . The upper (lower) sign in Eq. (26) applies if the uncoupled bound hole excitation is even (odd), but  $\sin[\delta_e^{\text{bg}}(k) - \delta_0^{\text{bg}}(k)] \approx 0$  and the first term in Eq. (26) dominates. The Green's function of Eq. (20) is

$$G_k(x, s) = \frac{M}{\hbar^2 W_k} \times \begin{cases} \psi_k^e(x) \psi_k^o(s) - \psi_k^o(x) \psi_k^e(s), & x > s \\ \psi_k^o(x) \psi_k^e(s) - \psi_k^e(x) \psi_k^o(s), & x < s \end{cases}. \quad (27)$$

In the limit  $\Delta(x) \rightarrow 0$ ,  $\chi(k) = 0$  and the resonances occur for  $\epsilon_k^0 = \epsilon_b^0$ , i.e., the quasiparticle energy of the bound hole excitation matches the quasiparticle energy of the scattering particle excitation. The resonance energy is well approximated by  $E_k = E_r^b$  [see Eq. (23)], as indicated by the vertical lines in Fig. 4(b).

The energy  $E_r^b$  can be interpreted as the energy required to excite a bound particle to the chemical potential and to create a second particle at the chemical potential with opposite spin. A scattering resonance occurs near this energy if there is coupling between the scattering state and the intermediate state, where the projectile particle and the bound particle of opposite spin form a pair at the chemical potential. In general, this intermediate state is forbidden because the chemical potential is not an energy eigenvalue of Eq. (20). However, in the mean-field theory, the pair potential  $\Delta(x)$  facilitates pair creation and destruction as if there is a source/sink of atom pairs at the chemical potential, i.e., there is an effective pair condensate at  $\mu$ . These *pairing vibrations* [13,27] allow the projectile particle and a bound particle of opposite spin to be simultaneously removed from the system, and the intermediate state for the scattering process is a bound hole excitation with two fewer particles than the scattering state [see Figs. 3(b) and 3(c)]. In a number-conserving treatment, coupling to this intermediate state would be forbidden because Hamiltonian (1) does not couple states with different numbers of particles.

We conclude that, in this case, the scattering resonances predicted by the mean-field approach are spurious. In particular, the mean-field theory does not conserve particle number and this allows for coupling between sectors of the Hilbert space corresponding to different numbers of particles. We discuss the validity of the BCS mean-field approach in more detail in the following section.

## V. VALIDITY OF MEAN-FIELD THEORY

The conventional application of BCS mean-field theory provides a steady-state ansatz for the quantum system. This BCS state, introduced in 1957 by Bardeen, Cooper, and Schrieffer [28], is not an eigenstate of the total number of particles in the system, but it can be used to compute the expectation values of a variety of physical observables, in

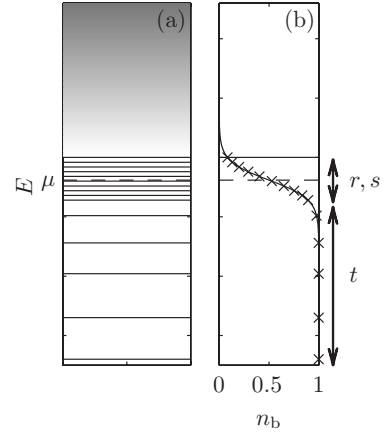


FIG. 5. (a) The energy-level diagram for a generic quantum system for which the energy levels near the chemical potential are highly degenerate. (b) The average energy-level population  $n_b$  that could be expected from a BCS mean-field calculation. In both panels, the dashed horizontal line indicates the chemical potential  $\mu$ .

particular, the number-conserving Hamiltonian. It can be shown that the expectation value of any number-conserving operator will yield approximately the same result when evaluated either with the BCS state or with the projection of that state on any eigenstate of the total number of particles, so long as it has a particle number eigenvalue close to the (large) mean particle number in the BCS state [22].

Our use of BCS theory is less well justified because, rather than investigating the full number-conserving Hamiltonian [Eq. (1)] within the BCS ansatz, we address the dynamics governed by the approximate number nonconserving Hartree-Fock-Bogoliubov Hamiltonian [Eq. (17)]. Higher-order methods based on the number-conserving Hamiltonian have been applied to scattering from nuclei (e.g., [29]). However, in the case of our one-dimensional scattering problem, the spurious scattering resonances described in Sec. IV are retained even in such a treatment.

It is well known that the BCS mean-field approach is particularly prone to giving inaccurate results when applied to small systems. So, it is perhaps not surprising that the BCS treatment predicted spurious resonances in Sec. IV. However, by illustrating in detail the nature of this breakdown of the theory, we can now present arguments for why the BCS method can be expected to give accurate predictions in higher dimensions and for larger systems.

One of the difficulties with using the BCS mean-field approach to describe the one-dimensional scattering problem is that the chemical potential is not, in general, an allowed energy level in the system. However, this problem only arises in systems with discrete energy levels. For example, in two or three dimensions where the energy levels can be highly degenerate, or in a homogeneous system where the energy spectrum is continuous, the chemical potential is far more likely to lie at, or very near to, an available energy level. Furthermore, the high degeneracy provides a compelling argument for the validity of the mean-field description in the macroscopic limit, as discussed below.

Figure 5(a) represents the excitation spectrum for a generic quantum system where the energy levels are highly

degenerate near the chemical potential. Applying the BCS mean-field theory to such a system would give an energy-level average population  $n_b$  that varies slowly across the quasicontinuum, as indicated in Fig. 5(b). Calculating the scattering properties of the system, in the mean-field approach, we would expect to find scattering resonances at energies  $E_k \approx E_r^b$  for each sufficiently low-lying energy level (i.e., for  $E_b < 2\mu$ ). To determine whether this is reasonable, we could alternatively consider this system in the spirit of the configuration-interaction approach of Sec. III. In this treatment we would expect there to be a large number of resonances due to the many possible  $(r, s, t)$  configurations. In particular, many resonances for a given value of  $t$  would have similar resonance energies and, taking the continuum limit for the  $r$  and  $s$  levels, these resonances would overlap and we would predict essentially the same result as in the BCS mean-field treatment, i.e., a single resonance for every low-lying bound state  $t$ . To verify this quantitatively, it would be necessary to show that the operator  $\hat{a}_{r\uparrow}^\dagger \hat{a}_{s\downarrow}^\dagger$  in Eq. (9) could be replaced by a complex number that was approximately independent of  $r$  and  $s$  in the quasicontinuum. Therefore, Eq. (9) could be reinterpreted in the spirit of the Bogoliubov transformation (18).

To rephrase the argument, consider a group of  $\mathcal{N}$  states near the chemical potential that are on average half filled. In this case the states near the chemical potential are mutually coupled by the many-body pairing and the corresponding eigenstates can be assumed to be essentially symmetric in terms of the population of each single-particle state. The probability of transferring the projectile particle, and a low-lying bound particle of opposite spin, to any of the half-filled levels is then amplified by a combinatorial factor increasing with  $\mathcal{N}$ , similar to the collective spontaneous emission (Dicke super-radiance) of light from a symmetrically excited atomic medium [30]. The collective enhancement would be maximum at exactly half filling, and the intermediate states populating  $r$  and  $s$  levels near  $\mu$  would yield one strong resonance for every level  $t$ , in agreement with the BCS mean-field prediction. In this regime the pairing vibrations, corresponding to correlated pairs being added to and removed from the system, become collective and can be described by a classical field [13,27]. Additional resonances due to unpopulated  $r$  and  $s$  levels lying well above the chemical potential (as in Fig. 2) do not benefit from the collective enhancement associated with the half filling of levels and would be comparatively unimportant in the macroscopic limit. This justifies the use of the self-consistent mean-field treatment as a symmetry-breaking approach in the

same spirit that the semiclassical approximation with a mean collective dipole is applied to the description of optical super-radiance. A similar interpretation has been discussed in the context of open quantum billiards [31,32] and nuclear reactions [33,34].

## VI. CONCLUSION

We have considered single-particle scattering from a trapped two-component degenerate Fermi gas when the projectile particle is identical to one of the confined species. Our theoretical treatment is based on a configuration-interaction approach and we predict Fano-type scattering resonances that are possible because of interatomic pairing. The scattering resonances are sensitive to the ground-state properties of the trapped Fermi gas and we have described the key features of the scattering resonances quantitatively.

We have also presented a BCS mean-field approach to the scattering problem and have shown that the non-number conservation of the theory leads to spurious scattering resonances. We have described in detail the breakdown of BCS theory for this case but have argued that in macroscopic systems where the energy spectrum is highly degenerate, or continuous, the BCS theory may be expected to give accurate results. Furthermore, we have suggested that the BCS mean-field approximation can be interpreted as an effective semiclassical representation of super-radiance in the system, and this presents an interesting avenue for further research.

The scattering resonances we predict are relevant for a range of reflection and transmission experiments with cold atoms. In particular, the energy sensitivity of the scattering resonances could allow for energy filtering and, in the case of spin imbalance, spin filtering may also be possible. This is interesting in the context of cold atom chip experiments and recent theoretical proposals for developing cold atom analogs of electronic devices [35–37]. Indeed, Fano-type scattering resonances have been observed in a single-electron transistor [38], and the transport properties of different junction interfaces have been widely studied [39–41]. Finally, recent work has also shown that the scattering properties of normal-superfluid interfaces have implications when considering the thermodynamics of a Fermi gas [42].

## ACKNOWLEDGMENTS

The authors thank Stefan Rombouts for helpful discussions, and N.N. acknowledges financial support from the Danish Natural Science Research Council.

- 
- [1] S. Inouye, M. R. Andrews, J. Stenger, H.-J. Miesner, D. M. Stamper-Kurn, and W. Ketterle, *Nature (London)* **392**, 151 (1998).  
 [2] S. Jochim, M. Bartenstein, A. Altmeyer, G. Hendl, S. Riedl, C. Chin, J. Hecker Denschlag, and R. Grimm, *Science* **302**, 2101 (2003).

- [3] C. A. Regal, C. Ticknor, J. L. Bohn, and D. S. Jin, *Nature (London)* **424**, 47 (2003).  
 [4] M. W. Zwierlein, J. R. Abo-Shaer, A. Schirotzek, C. H. Schunck, and W. Ketterle, *Nature (London)* **435**, 1047 (2005).  
 [5] C. Chin, M. Bartenstein, A. Altmeyer, S. Riedl, S. Jochim, J. Hecker Denschlag, and R. Grimm, *Science* **305**, 1128 (2004).

- [6] U. V. Poulsen and K. Mølmer, *Phys. Rev. A* **67**, 013610 (2003).
- [7] M. Grupp, G. Nandi, R. Walser, and W. P. Schleich, *Phys. Rev. A* **73**, 050701(R) (2006).
- [8] H. Moritz, T. Stöferle, K. Günter, M. Köhl, and T. Esslinger, *Phys. Rev. Lett.* **94**, 210401 (2005).
- [9] T. Kinoshita, T. Wenger, and D. S. Weiss, *Nature (London)* **440**, 900 (2006).
- [10] J. Billy, V. Josse, Z. Zuo, A. Bernard, B. Hambrecht, P. Lugan, D. Clément, L. Sanchez-Palencia, P. Bouyer, and A. Aspect, *Nature (London)* **453**, 891 (2008).
- [11] T. Weber, J. Herbig, M. Mark, H.-C. Nägerl, and R. Grimm, *Science* **299**, 232 (2003).
- [12] M. Grasso, N. Sandulescu, N. Van Giai, and R. J. Liotta, *Phys. Rev. C* **64**, 064321 (2001).
- [13] P. Ring and P. Schuck, *The Nuclear Many-Body Problem* (Springer-Verlag, Berlin, 2004).
- [14] G. M. Bruun and K. Burnett, *Phys. Rev. A* **58**, 2427 (1998).
- [15] We assume that the continuum modes do not contribute to the bound component of the excitation, i.e., that the Hartree-Fock method gives a good description of the single-particle bound-state energy levels of the system.
- [16] E. P. Wigner and L. Eisenbud, *Phys. Rev.* **72**, 29 (1947).
- [17] U. Fano, *Phys. Rev.* **124**, 1866 (1961).
- [18] A. Bulgac, preprint FT-194-1980, Central Institute of Physics, Bucharest, 1980; e-print arXiv:nucl-th/9907088.
- [19] S. T. Belyaev, A. V. Smirnov, S. V. Tolokonnikov, and S. A. Fayans, *Sov. J. Nucl. Phys.* **45**, 783 (1987).
- [20] J. Dobaczewski, W. Nazarewicz, T. R. Werner, J. F. Berger, C. R. Chinn, and J. Dechargé, *Phys. Rev. C* **53**, 2809 (1996).
- [21] The Hartree-Fock-Bogoliubov ground state is used when evaluating matrix elements in the mean-field approach. Therefore, the Hartree potential  $U(x)$  in the Hartree-Fock-Bogoliubov treatment is not identical to the Hartree potential  $W(x)$  in the Hartree-Fock treatment.
- [22] P. G. de Gennes, *Superconductivity of Metals and Alloys* (W. A. Benjamin, New York, 1966).
- [23] The energy eigenvalues  $E_n$  of Eq. (20) are not quantitatively identical to the energy eigenvalues of Eq. (6).
- [24] H. Friedrich, *Theoretical Atomic Physics* (Springer-Verlag, Berlin, 1991).
- [25] We have chosen  $\Delta(x)$  and the eigenstates  $\psi_n(x)$  of Eq. (20) to be real.
- [26] G. B. Arfken and H. J. Weber, *Mathematical Methods for Physicists*, 4th ed. (Academic Press, California, 1995).
- [27] A. Bohr and B. R. Mottelson, *Nuclear Structure* (W. A. Benjamin, Massachusetts, 1975), Vol. II.
- [28] J. Bardeen, L. N. Cooper, and J. R. Schrieffer, *Phys. Rev.* **108**, 1175 (1957).
- [29] S. E. A. Orrigo, H. Lenske, F. Cappuzzello, A. Cunsolo, A. Foti, A. Lazzaro, C. Nociforo, and J. S. Winfield, *Phys. Lett. B* **633**, 469 (2006).
- [30] R. H. Dicke, *Phys. Rev.* **93**, 99 (1954).
- [31] R. G. Nazmitdinov, K. N. Pichugin, I. Rotter, and P. Šeba, *Phys. Rev. E* **64**, 056214 (2001).
- [32] R. G. Nazmitdinov, K. N. Pichugin, I. Rotter, and P. Šeba, *Phys. Rev. B* **66**, 085322 (2002).
- [33] N. Auerbach and V. Zelevinsky, *Nucl. Phys. A* **781**, 67 (2007).
- [34] A. Volya and V. Zelevinsky, *Nucl. Phys. A* **788**, 251c (2007).
- [35] B. T. Seaman, M. Krämer, D. Z. Anderson, and M. J. Holland, *Phys. Rev. A* **75**, 023615 (2007).
- [36] R. Walser, E. Goldobin, O. Crasser, D. Koelle, R. Kleiner, and W. P. Schleich, *New J. Phys.* **10**, 045020 (2008).
- [37] J. Y. Vaishnav, J. Ruseckas, C. W. Clark, and G. Juzelūnas, *Phys. Rev. Lett.* **101**, 265302 (2008).
- [38] J. Göres, D. Goldhaber-Gordon, S. Heemeyer, M. A. Kastner, H. Shtrikman, D. Mahalu, and U. Meirav, *Phys. Rev. B* **62**, 2188 (2000).
- [39] S. Das, S. Rao, and A. Saha, *Europhys. Lett.* **81**, 67001 (2008).
- [40] M. S. Kalenkov and A. D. Zaikin, *Phys. Rev. B* **75**, 172503 (2007).
- [41] J. Demers and A. Griffin, *Can. J. Phys.* **49**, 285 (1971).
- [42] B. Van Schaeybroeck and A. Lazarides, *Phys. Rev. Lett.* **98**, 170402 (2007).